



Controlling the rf phase error induced micromotion in Paul trap

Ting Chen¹ · Wei Wu¹ · Yi Xie¹ · Jie Zhang¹ · Baoquan Ou¹ · Chunwang Wu¹ · Pingxing Chen¹

Received: 13 November 2019 / Accepted: 24 April 2020 / Published online: 15 May 2020
© Springer-Verlag GmbH Germany, part of Springer Nature 2020

Abstract

Excess micromotion of trapped ions leads to several adverse effects, such as modulating the absorption spectrum, shifting the transition frequency, and causing extra motional heating of ions. Moreover, it is hard to deal with, if there is no rf null point in a Paul trap. In this paper, two methods are proposed to control these adverse effects introduced by excess micromotion. The first method can eliminate the spectral modulation effect while keeping the micromotion unaffected by phase modulating the related laser. The second one can control the amplitude of micromotion or compensate it completely to remove the frequency shift effects by applying ac voltage to the dc electrodes. With these two methods, we are not only able to control the micromotion amplitude in a Paul trap without rf null point, but also to realize effective sideband cooling and quantum state manipulating when ions still undergo large excess micromotion.

1 Introduction

The excess micromotion of ions in a radio frequency (rf) trap has gained much attention from researchers on optical frequency standards [1, 2], quantum computing [3–6], and other related high-precision measurement [7, 8]. That is mainly because the excess micromotion will lead to some adverse effects: (1) extra ac-stark shift and second-order Doppler shift will arise [9], which will greatly affect the accuracy of optical frequency standard system. (2) The absorption spectrum will be affected [9, 10]: for the transition whose natural linewidth is comparable or wider than the micromotion frequency, the absorption spectrum will be broadened, which leads to ion heating (cooling) effect when the laser frequency is in red (blue) detuning range [11]. On the contrary, if natural linewidth of the transition is much narrower than the micromotion frequency, then the micromotion sideband is resolvable, the carrier transition will be remarkably weakened. (3) The micromotion may lead to additional heating to the motional state of trapped ions,

especially for large number of not-so-cold ions [12–15]. Nevertheless, the non-uniformly distributed Rabi frequencies induced by micromotion were utilized to realize quantum state entanglement [16] and single ion addressing [17, 18]. What is more, a scheme was even proposed to improve both the fidelity and speed of the quantum logic gates by utilizing the micromotion [6]. Therefore, controlling the excess micromotion is very important for the application of trapped ions.

Detailed analysis of excess micromotion has been presented for two decades. The detection methods of micromotion include rf-photon correlation [9], sideband spectrum detection, pulsed spectroscopy [10], ion-trajectory analysis [19], and so on. Excess micromotion can be classified into two types. One is induced by stray electric field near the trap center which pushes the ion away from the rf null position of the ac electric field. This type of micromotion can be well compensated using a dc voltage to push the ion back to the nodal position. The other type originates from the absence of rf null point in some specific traps, which may come from the asymmetry of rf electrodes or the rf phase mismatch between them. This kind of micromotion is collectively referred as phase error excess micromotion (PEEM) in the following, which could be very remarkable in amplitude and can't be compensated by a dc voltage.

In this paper, we propose two methods to control the effect of PEEM with experimental demonstration. First, we demonstrate that the spectral modulation effect of PEEM can be compensated by inverse modulating the phase of the interacting

Ting Chen and Wei Wu contributed equally to this work.

✉ Yi Xie
xieyi2015@nudt.edu.cn

✉ Pingxing Chen
pxchen@nudt.edu.cn

¹ Department of Physics, College of Liberal Arts and Sciences, National University of Defense Technology, Changsha 410073, Hunan, China

laser. Although the excess micromotion still exists physically, the phase-modulation effect of the interacting laser is eliminated. This method can be applied in experiments to measure the spectral in the presence of PEEM or to explore the motional effect of the micromotion. Second, a large amplitude PEEM in the axial direction in a linear trap is well compensated by adding a proper ac voltage to the end-cap electrodes. This method eliminates the PEEM-induced ac-stark shift and second-order Doppler shift; therefore, it should be useful for quantum information processing and quantum precision measurement applications. Using these two techniques, the source of the axial PEEM in our linear trap is analyzed and the heating effect of rf on a single cold-trapped ion is measured.

2 Eliminating the micromotion-induced laser-phase-modulation effect

Considering an ion undergoes rf-driven excess micromotion whose amplitude and frequency are much larger than those of the secular motion, the ion’s displacement x can be expressed as

$$x = a \sin(\Omega t + \phi_{rf}), \tag{1}$$

where a and Ω are the amplitude and frequency of the micromotion, respectively, ϕ_{rf} is the phase of ion’s motion. We assume that the electric field of the interacting laser has amplitude E_0 , frequency ω , phase ϕ_l , and wave vector \mathbf{k} . For simplicity, we also assume that the laser wave vector takes the x -direction. The electric field of this laser can be expressed as

$$E = \text{Re}(E_0 \exp(i(\omega t - kx + \phi_l))). \tag{2}$$

In the rest frame of an ion undergoing excess micromotion, the laser field can be expressed as

$$E' = \text{Re}\{E_0 \exp[i(\omega t - ka \sin(\omega t + \phi_{rf}) + \phi_l)]\}. \tag{3}$$

Therefore, the laser is phase modulated by the ion’s excess micromotion. This will lead to many spectral effects such as adding spectral sidebands to an electric quadruple transition or broadening the absorption spectrum of an electric dipole transition, which will complicate the heating rate measurement based on Doppler recooling method [20, 21]. To compensate for the micromotion-induced laser-phase-modulation effect, we modulate the phase ϕ_l of the laser beam as $m \sin(\Omega t + \phi_m)$, and the laser’s field is turned into

$$\begin{aligned} E' &= \text{Re}\{E_0 \exp[i(\omega t - ka \sin(\omega t + \phi_{rf}) + m \sin(\Omega t + \phi_m))]\}, \\ &= \text{Re}\{E_0 \exp[i(\omega t + \beta_s \sin(\Omega t + \phi'))]\}. \end{aligned} \tag{4}$$

Here the phase ϕ' is not concerned and the spectral modulation index β_s can be expressed as

$$\beta_s = \sqrt{m^2 + k^2 a^2 - 2mka \cos(\phi_m - \phi_{rf})}. \tag{5}$$

When $\beta_s = 0$, the spectral modulation effect of ion’s micromotion will be eliminated even though the excess micromotion still exist. This can be easily realized by choosing the modulation phase $\phi_m = \phi_{rf}$ and modulation amplitude $m = ka$. If $\beta_s \neq 0$, according to the Bessel function expansion, the spectrum can be expressed as:

$$\begin{aligned} &E_0 \exp[i(\omega t + \beta_s \sin(\Omega t + \phi))] \\ &= E_0 \exp(i\omega t) \sum_{n=-\infty}^{\infty} J_n(\beta_s) \exp[in(\Omega t + \phi)]. \end{aligned} \tag{6}$$

Therefore, by introducing a phase modulation to the laser field, the spectral sidebands are now determined by the spectral modulation index β_s rather than micromotion modulation index introduced in [9]. This equation shows the energy distribution among different spectrum lines, and also determines the transition strength for the i th order of micromotion sidebands by $\Omega_i^{\text{rabi}} = \mu E_0 J_i(\beta_s) / \hbar$. Using this relation, the spectral modulation index β_s can be determined experimentally, by measuring the Rabi frequencies of the carrier transition and several orders of micromotion sideband.

In our experiment, a $^{40}\text{Ca}^+$ ion is confined in a blade-shaped trap. The absorption spectrum of transition $S_{1/2} \leftrightarrow D_{5/2}$ is measured by electron shelving technology [22]. Due to the geometric defects of the trap, axial PEEM still exists after optimizing compensation voltages of the radical dc electrodes. An electro-optic modulator (EOM) is used to modulate the phase of 729-nm laser beam and compensate for the micromotion-induced laser-phase-modulation effect. The transition strengths of micromotion sidebands are reduced from a higher order to the lowest one successively, by carefully adjusting the amplitude and phase of the modulation signal. Under the optimal parameters, i.e. $m = ka$ and $\phi_m = \phi_{rf}$, the spectral modulation index β_s can be suppressed to around 0.05. By varying ϕ_m between 0 and π , the spectral modulation index β_s can be adjusted from 0 to $2ka$, according to Eq. (5). In this way, we have measured the transition strengths of the carrier and several micromotion sidebands of the lowest order with different β_s . The result is shown in Fig. 1a. It is in good agreement with the theoretical value of the Bessel function expansion, with the free parameters $\mu E_0 / \hbar$, $m = ka$ and $(\phi_m - \phi_{rf})$ being derived by optimal fitting all the measured data. The calculated β_s by optimal fitting is also shown in Fig. 1b with respect to the rf phase. Under the optimal parameters, the micromotion sidebands are almost completely eliminated, indicating that the spectrum modulation effects of PEEM is greatly suppressed in this transition. According to the experimental data,

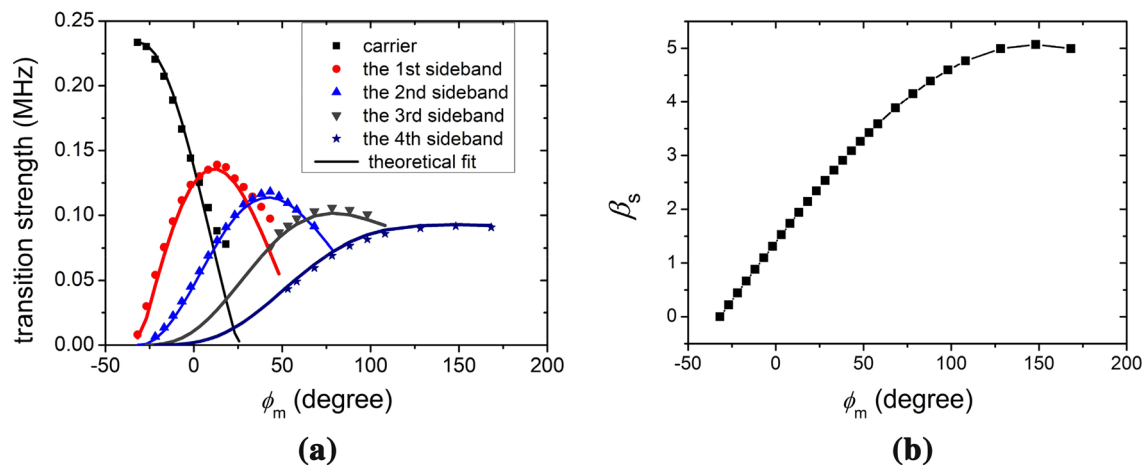


Fig. 1 Controlling the spectral modulation effect by varying the EOM modulation phase. **a** The Rabi frequencies of the carrier and sidebands vary with the modulation phase. The dots on the graph represent the measured data, and the solid lines represent the best fit for all the measured data with the laser intensity, rf phase, and the micro-

motion modulation index being fitted parameters. Black (red, blue, brown, and purple) lines and dots correspond to carrier (the first to fourth order sidebands) transition. **b** The relationship between spectral modulation index β_s and the rf phase. The squares are calculated with data in **a** and the solid line is the best fit

the amplitude of the PEEM is as large as 290 nm, corresponding to a micromotion modulation index of 2.5, which means that the energy of carrier component occupies only less than 5% of the total energy. In such a condition, we still accomplished resolved sideband cooling in this direction to a 98% ground state population and recovered the carrier transition to nearly 100% of the total energy, by phase modulating the sideband cooling laser.

This technology makes it possible for many experiments, especially for those that cannot be realized in the presence of large micromotion. For example, effective sideband cooling and practical quantum operation [23], which previously could not be realized in the case of large amplitude PEEM, for the strong coupling strength needed is weakened by micromotion modulation, can be realized now by phase modulating the interacting laser field. What's more, since the phase modulation is realized by EOM, the switching between different modulation depths can be performed very fast. This may find applications in large-scale quantum simulation using planar ion crystal [4, 24, 25]. In such a case, each ion has different distances away from trap axis and, therefore, has different micromotion amplitudes and phases. This method allows us to operate every specific ion with different laser modulation parameters.

Although our experiment is realized with electric quadrupole optical transition, this technique can also be applied to other transitions such as magnetic dipole transition and electric dipole transition. The latter is widely used in Doppler cooling, and the laser phase-modulation method can eliminate the PEEM-induced linewidth broadening and restore the cooling efficiency. In addition, when the heating

rate is measured by Doppler recooling method, the difficulty of spectrum shape distortion caused by PEEM [20] can also be overcome.

3 Eliminating the PEEM by ac voltage counter driving

In the previous section, we have discussed the elimination of the excess micromotion-induced phase-modulation effect; however, the trapped ion still undergoes micromotion in reality. In this section, we will introduce a method to minimize the PEEM amplitude of an ion in the axial direction.

The method is demonstrated with the setup shown in Fig. 2a. The frequency of the ac voltage source (oscillator) is set exactly equal to that of the trap rf (13.6 MHz). The phase of the oscillator is referenced to the trap rf signal. After power amplifying, it is coupled to the end caps by LC resonant circuit. This signal forces the ion to vibrate the same way as excess micromotion with the amplitude proportional to the amplitude of ac voltage. Let us assume that in the absence of micromotion, the amplitude and phase of the vibration driven by this ac voltage are b and ϕ_{ac} , the final micromotion modulation index can be derived the same way as Eq. (5):

$$\beta_m = k\sqrt{a^2 + b^2 - 2abc\cos(\phi_{ac} - \phi_{rf})}. \quad (7)$$

By appropriately choosing relative phase and amplitude of the rf signal, the forced motion will cancel the excess micromotion, leading to $\beta_m = 0$. Otherwise, by varying the

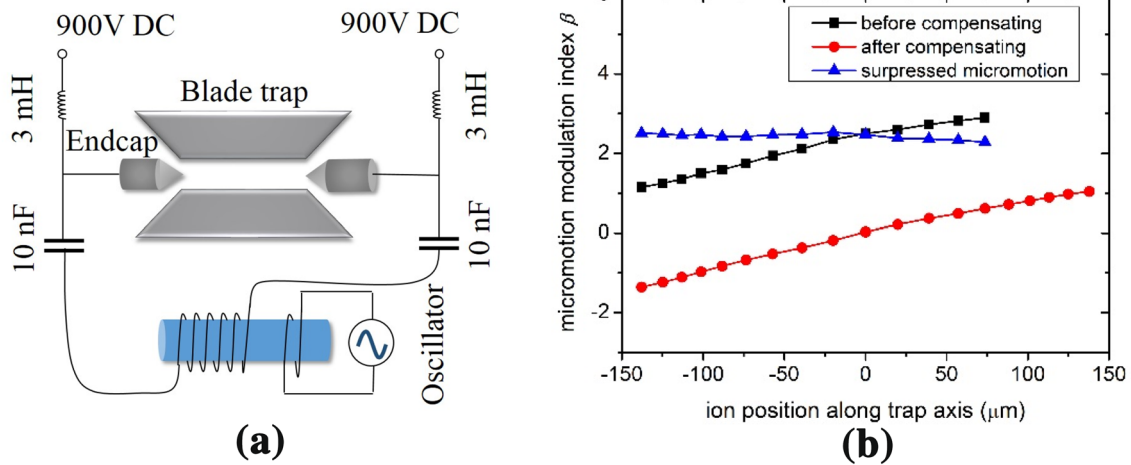


Fig. 2 **a** Experimental setup of the PEEM controlling. Phase of the oscillator is referenced to the trap rf signal and the amplitude and phase are adjustable. **b** The micromotion amplitudes at different positions measured by moving ions along the trap axis. Data measured

before and after the PEEM compensating are represented by black squares and red circles, respectively, and negative value means opposite phase. The blue triangles represent the differences between the measured data before and after compensating

phase of the ac signal on end caps, the final micromotion modulation index β_m can be adjusted from 0 to twice of the unaffected one.

In this experiment, 1.4 MHz trap frequency is achieved by applying around 900 V dc voltages to the end caps. After power amplifying, an ac signal with adjustable amplitude and phase is coupled to the end caps through a resonator. The overall voltage gain is about 50 dB. When the amplitude of the ac signal source is about 0.25 vrms and its phase is opposite to that of the micromotion, the micromotion sideband almost disappears. The residual micromotion modulation index β_m is as low as 0.05, which corresponds to an oscillation amplitude of 5.8 nm.

To explore the spatial characteristics of the PEEM in the axial direction, we move the ion along the trap axis for about 250 μm away from the trap center by varying dc voltage on one end cap, and the micromotion modulation index is measured at several locations with the method mentioned in the previous section. At first, the ac compensation voltage is turned off, the measured curve shows a monotonous profile and no rf null point is found, as is shown in Fig. 2b marked with black square. Then the ac compensation voltage is turned on and the parameters are optimized to compensate for the micromotion of ion at the trap center. The residual micromotion modulation index is measured again for ions at different positions along the trap axis. The measured data is shown in Fig. 2b marked with red circle. We found the difference of the β_m between these two cases have no obvious spatial heterogeneity. Since the difference is proportional to the compensation effect provided by ac compensation voltage, it can be concluded that the compensation or driving

effect of ac voltage on the end caps is nearly uniform for the center positions.

Therefore, we deduce that the inhomogeneous distribution of micromotion amplitude is most probably caused by blade electrodes due to their imperfect shape or assembly error, because they are closer to the trap center than the end caps. The inhomogeneous distribution is not necessarily all disadvantages, they also can be used to address a single ion in a string [17, 18].

Compensating for the PEEM by applying ac voltage to electrodes has the advantage over laser-phase-compensation method that the micromotion is truly compensated; therefore, the accompanied ac-stark shift and second-order Doppler shift can be overcome, which is very important for precision measurement applications with trapped ion. In addition, β_m can be adjusted by only changing the phase, which provides us an opportunity to investigate the dynamics of trapped ions under large micromotion amplitude. However, since the micromotion is not uniform along the trap axis, the laser-phase-compensation method together with single-ion addressing method still plays an irreplaceable role in quantum operations.

4 Measuring the heating rate under large ion micromotion

Heating rate is one of the most concerned features in a quantum information processing oriented ion trap, which limits the coherence time of a motional state and the fidelity of a quantum logic gate [26]. The heating effect mainly comes

from the electrical noise near the trap, but may also be introduced by rf field.

Numerical simulations based on ion cloud shows that the rf-induced heating effect depends greatly on the temperature of trapped ions, and the heating effect is negligible when the effective temperature of the trapped ions is below 0.5 K [14]. Since the collision between ions is the major source of rf heating for an ion cloud, situation is quite different for a single trapped ion. However, additional heating effect may still exist if there are kinetic energy exchange channels between micromotion and secular motion such as nonlinear resonance [27]. However, to verify this in experiment is difficult, because neither of the two main methods for measuring the heating rate is applicable in the case of larger micromotion amplitude. One method is to measure the increasing rate of mean phonon number by fitting the Rabi flopping curve of the blue sideband transition after the ion being cooled to ground state [23]. This method relies greatly on the transition strengths of carrier and secular-motion sidebands, and, therefore, lost its measurement accuracy or even cannot be accomplished due to laser-phase-modulation effect of PEEM. The other method is the so-called Doppler recooling method, which is to obtain the mean phonon number by fitting the emitted fluorescence during Doppler recooling process after the ion has been heated up far beyond the ground state [28]. This method relies on the fluorescence emitting law, which will be greatly affected by the combined effect of the micromotion and Zeeman splitting under moderate magnetic field. Therefore, the complicated deformation of absorption spectrum with multi-level energy structure have to be considered [21].

Here, we are able to solve these problems by the combination of the aforementioned two methods. The process is shown in Fig. 3a. First, we compensate for the micromotion of a single $^{40}\text{Ca}^+$ by applying proper ac signal to end caps. Secondly, the micromotion modulation index is controlled between 0 and $2ka$ by varying the phase of the ac modulation signal within π . Controlling the micromotion amplitude by varying the phase rather than the amplitude of rf signal removes the possibility of heating rate variation due to rf power induced electrode temperature variation. In this way, the only possible factor of the heating rate variation is the varied excess micromotion amplitude. Then, the mean phonon number is cooled down to less than 0.2 by Doppler cooling and sideband cooling for each experiment run. This cooling limit is basically limited by the reduced Doppler cooling efficiency under large PEEM, since our Doppler cooling laser is not phase modulated by EOM. After that, all the lasers are blocked for a variable time duration, and the ion will be heated up gradually. At the last step, the Rabi oscillation of the blue sideband transition is recorded to obtain the mean phonon number. In both steps of sideband cooling and phonon number measurement, the phase-modulation effect of the sideband driving laser is well compensated by a phase-modulation EOM.

The result is shown in Fig. 3b. It shows that heating rate of a single ion in our trap has no significant relationship with the ion's micromotion with the modulation index up to 3.5. This experiment is restricted to the parameter region where micromotion modulation index is less than 3.5 (micromotion amplitude is about 406 nm). Because our Doppler cooling lasers are not phase compensated, the broadened absorption spectrum cannot provide sufficient Doppler cooling

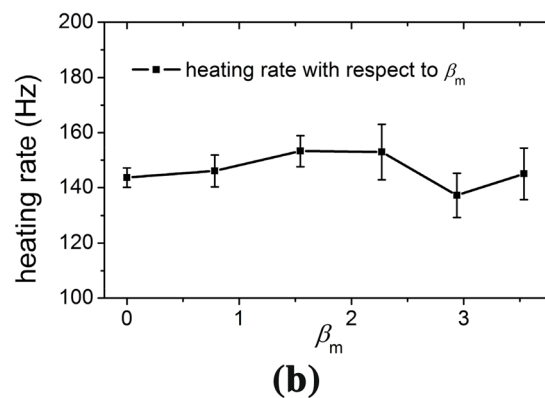
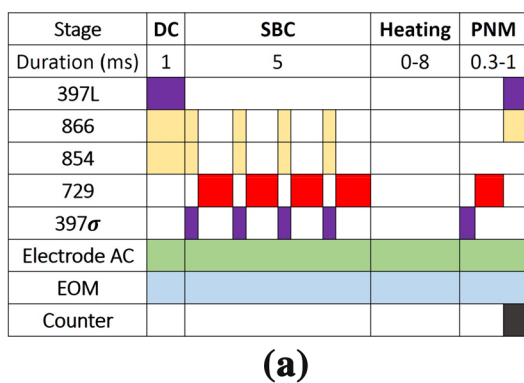


Fig. 3 Measurement of the relationship between heating rate and micromotion amplitude. **a** The experimental time sequence (DC, SBC, PNM are abbreviations of Doppler cooling, sideband cooling and phonon number measurement, respectively. The 397L, 866, 854, 729, and 397 σ represent corresponding laser beams). The ac voltage on electrode and EOM phase modulation are all kept on during the whole experiment. The counter is used to count the photon number within 0.3 ms at the PNM stage. For each experimental run, the

micromotion amplitude is controlled and varied by tuning the phase of ac voltage on electrode. Meanwhile, the phase and amplitude of the EOM driver are well calibrated to cancel the spectral modulation effect of the 729 nm laser. The duration of heating stage is swept from 0 to 8 ms to derive the heating rate. **b** Results of the measurement, where the error bars are origin from fitting errors of the PNM data

efficiency to reach the Lamb–Dick region and the sideband cooling fails. However, it is not a fundamental limit, further investigation could be accomplished with simultaneously phase-compensated Doppler cooling lasers. Besides, phase-compensated Doppler cooling lasers can also find applications in fast measurement of the heating rate in a surface electrode trap where the Doppler recoiling method is preferred.

5 Conclusion and discussions

In our paper, two methods which can eliminate the adverse effects of PEEM in a Paul trap have been experimentally demonstrated. The laser-phase-compensation method enables us to accomplish effective sideband cooling and quantum state operation in the presence of large micromotion, which makes it possible to effectively manipulate the quantum state of a single ion in a planar ion crystal. Besides, the Doppler recoiling method to measure the heating rate in ion traps can now be conveniently extended to the case where the PEEM cannot be compensated. Although the experiment is demonstrated on a narrow optical quadruple transition, this method is generic and should also work for other optical- or microwave-driven transitions. Another method to compensate for the PEEM itself by adding ac voltage to the electrodes can remove the PEEM accompanied ac-stark shift and second-order Doppler shift. It can be applied in precision measurements. Moreover, the amplitude of micromotion can be adjusted without changing the ion position or the power of compensation ac voltage. These two methods allow us to investigate the difference of ion's dynamics with or without PEEM. As an example, we measured the heating rate with a single cold ion of different PEEM amplitude, no significant heating effect related to PEEM is found. It is worth mentioning that these two methods provide tools to fully control the PEEM and facilitate the utilizing of micromotion to improve the quantum logic gates [6].

Acknowledgements This work is supported by the National Key Research and Development Program under Grant no. 2016FA0301903, the Natural Science Foundation of China under Grant no. 11904402, and the Research Plan Project of National University of Defense Technology under Grants nos. ZK18-01-01 and ZK18-03-03.

References

1. J. Keller, H.L. Partner, T. Burgermeister, T.E. Mehlstäubler, J. Appl. Phys. **118**, 104501 (2015)
2. Y. Huang, H. Guan, P. Liu, W. Bian, L. Ma, K. Liang, T. Li, K. Gao, Phys. Rev. Lett. **116**, 013001 (2016)
3. C. Shen, L.M. Duan, Phys. Rev. A **90**, 022332 (2014)
4. S.T. Wang, C. Shen, L.M. Duan, Sci. Rep. **5**, 8555 (2015)
5. J.P. Gaebler, T.R. Tan, Y. Lin, Y. Wan, R. Bowler, A.C. Keith, S. Glancy, K. Coakley, E. Knill, D. Leibfried, D.J. Wineland, Phys. Rev. Lett. **117**, 060505 (2016)
6. A. Bermudez, P. Schindler, T. Monz, R. Blatt, M. Müller, New J. Phys. **19**, 113038 (2017)
7. G.P. Barwood, H.S. Margolis, G. Huang, P. Gill, H.A. Klein, Phys. Rev. Lett. **93**, 133001 (2004)
8. N.C. Lewty, B.L. Chuah, R. Cazan, B.K. Sahoo, M.D. Barrett, Phys. Rev. A **88**, 012518 (2013)
9. D.J. Berkeland, J.D. Miller, J.C. Bergquist, W.M. Itano, D.J. Wineland, J. Appl. Phys. **83**, 5025 (1998)
10. T. Pruttivarasin, M. Ramm, H. Häffner, J. Phys. B Atom. Mol. Opt. Phys. **47**, 135002 (2014)
11. J.I. Cirac, L.J. Garay, R. Blatt, A.S. Parkins, P. Zoller, Phys. Rev. A **49**, 421 (1994)
12. R.G. DeVoe, J. Hoffnagle, R.G. Brewer, Phys. Rev. A **39**, 4362 (1989)
13. S. Brouard, J. Plata, Phys. Rev. A **63**, 043402 (2001)
14. L.V. Ryjkov, X.Z. Zhao, H.A. Schuessler, Phys. Rev. A **71**, 033414 (2005)
15. C.B. Zhang, D. Offenberger, B. Roth, M.A. Wilson, S. Schiller, Phys. Rev. A **76**, 012719 (2007)
16. Q.A. Turchette, C.S. Wood, B.E. King, C.J. Myatt, D. Leibfried, W.M. Itano, C. Monroe, D.J. Wineland, Phys. Rev. Lett. **81**, 3631 (1998)
17. D. Leibfried, Phys. Rev. A **60**, R3335 (1999)
18. N. Navon, S. Kotler, N. Akerman, Y. Glickman, I. Almog, R. Ozeri, Phys. Rev. Lett. **111**, 073001 (2013)
19. T.F. Gloger, P. Kaufmann, D. Kaufmann, M.T. Baig, T. Collath, M. Johanning, C. Wunderlich, Phys. Rev. A **92**, 043421 (2015)
20. N. Daniilidis, S. Narayanan, S.A. Möller, R. Clark, T.E. Lee, P.J. Leek, A. Wallraff, St Schulz, F. Schmidt-Kaler, H. Häffner, New J. Phys. **13**, 013032 (2011)
21. T. Sikorsky, Z. Meir, N. Akerman, R. Ben-shlomi, R. Ozeri, Phys. Rev. A **96**, 012519 (2017)
22. J.C. Bergquist, R.G. Hulet, W.M. Itano, D.J. Wineland, Phys. Rev. Lett. **57**, 1699 (1986)
23. C. Monroe, D.M. Meekhof, B.E. King, S.R. Jefferts, W.M. Itano, D.J. Wineland, Phys. Rev. Lett. **75**, 4011 (1995)
24. H. Kaufmann, S. Ulm, G. Jacob, U. Poschinger, H. Landa, A. Retzker, M.B. Plenio, F. Schmidt-Kaler, Phys. Rev. Lett. **109**, 263003 (2012)
25. B. Yoshimura, M. Stork, D. Dadic, W.C. Campbell, J.K. Freericks, EPJ Quant. Technol. **1**, 2 (2014)
26. M. Brownnutt, M. Kumph, P. Rabl, R. Blatt, Rev. Mod. Phys. **87**, 1419 (2015)
27. A.N. Kotana, A.K. Mohanty, Int. J. Mass Spectrom. **414**, 13 (2017)
28. R.J. Epstein, S. Seidelin, D. Leibfried, J.H. Wesenberg, J.J. Bollinger, J.M. Amini, R.B. Blakestad, J. Britton, J.P. Home, W.M. Itano, J.D. Jost, E. Knill, C. Langer, R. Ozeri, N. Shiga, D.J. Wineland, Phys. Rev. A **76**, 033411 (2007)

Publisher's Note Springer Nature remains neutral with regard to jurisdictional claims in published maps and institutional affiliations.